

Evolution of the Fermi surface and the oscillatory exchange coupling across Cr and Cr-based alloys

R. J. Hughes,¹ S. B. Dugdale,¹ Zs. Major,¹ M. A. Alam,¹ T. Jarlborg,² E. Bruno,³ and B. Ginatempo³

¹*H. H. Wills Physics Laboratory, University of Bristol, Tyndall Avenue, Bristol BS8 1TL, United Kingdom*

²*DPMC, University of Geneva, 24 quai Ernest Ansermet, CH-1211 Geneva 4, Switzerland*

³*Department of Physics, University of Messina, Salita Sperone 31, 98166 Messina, Italy*

(Received 27 January 2004; published 6 May 2004)

A comprehensive investigation of the Fermi surface topologies of a series of $\text{Cr}_{1-x}\text{V}_x$ and $\text{Cr}_{1-x}\text{Mo}_x$ alloys highlights the role of nesting in determining the periods of the oscillatory exchange coupling observed in multilayer systems. The long-standing controversy over the origin of the long-period oscillations across Cr and Cr-based alloys is resolved, with the evolution of one dimension of the N -hole ellipsoid Fermi surface sheet being directly associated with the evolution of the period.

DOI: 10.1103/PhysRevB.69.174406

PACS number(s): 78.70.Bj, 71.18.+y, 74.70.Ad

In recent years the oscillatory magnetic exchange coupling in multilayer systems (magnetic layers separated by thin nonmagnetic spacer layers) has generated intense research activity,¹ due to the “giant magnetoresistance” (GMR) (Ref. 2) observed in these materials, which makes them technologically relevant to the development of new magnetoresistive devices. The exchange coupling causes the magnetization vectors in each magnetic layer to oscillate between antiferromagnetic and ferromagnetic alignments, with a periodicity that depends on the type and thickness of the material used in the intervening spacer layers. Spacer materials which show this behavior include transition metals, noble metals, and transition-metal alloys, with periods most commonly measured in the range 8–12 Å, except for Cr at ~ 18 Å in addition to a shorter period of ~ 4 Å.³ In this paper, we present the results of a comprehensive positron annihilation study which shows that the size of a particular feature in the Fermi surface (FS) of Cr known as the N -hole pocket (and its evolution under alloying with Mo and V) can be directly linked with the long-period oscillatory exchange coupling (OEC) in the Fe/Cr_{1-x}Mo_x/Fe and Fe/Cr_{1-x}V_x/Fe GMR systems.

While the details of the various theoretical approaches aimed at understanding this OEC can be broadly divided into Ruderman-Kittel-Kasuya-Yosida-based⁴ and quantum-well⁵ models, there is a general consensus that the phenomenon is associated with conduction electron spin-polarization “waves” governed by the FS of the spacer material. The oscillation periods λ are assumed to be directly connected to an extremal vector of length Q (perpendicular to the layers) in the (bulk) FS of the spacer metals ($\lambda = 2\pi/Q$), whereas the amplitude is believed to be a joint property of both the magnetic and the spacer layers.⁶ The short-period oscillation in Cr is thought to be associated with the “nesting” of the Γ -centered electron octahedron (see Fig. 1) and the H -hole octahedron (also the origin of the familiar spin-density wave in Cr, Ref. 7). However, the origin of the long-period oscillation has been a source of controversy,^{8–11} in that the periods are vastly different with Cr and isoelectronic Mo as spacer layers and that the period of oscillation reduces in the same fashion to the lower values for spacer layers of Cr-Mo

and Cr-V alloys with increasing Mo and V concentrations. Recent theoretical predictions have led to the common opinion that the long-range OEC with the transition metals and their alloys are driven by the ellipsoidal N -hole pockets,^{12–16} but an experimental verification of these has remained elusive until now. Given the sensitivity of the oscillation periods to extremal FS calipers and the acknowledged limitations of local-density approximation (LDA) calculations for the 3d transition series with respect to the relative positioning of the s - p and d states,¹⁴ experimental verification is essential. Principally owing to the lack of a suitable probe, the alloy FS topologies have not been previously measured.

The occupied momentum states, and hence the FS, can be accessed via the momentum distribution using the two-dimensional angular correlation of electron-positron annihilation radiation (2D-ACAR) technique.¹⁷ A 2D-ACAR measurement yields a 2D projection (integration over one dimension) of an underlying electron-positron momentum density, $\rho(\mathbf{p})$. In a metal, the presence of the FS is revealed by discontinuities in this distribution at the points $\mathbf{p}_F = (\mathbf{k}_F$

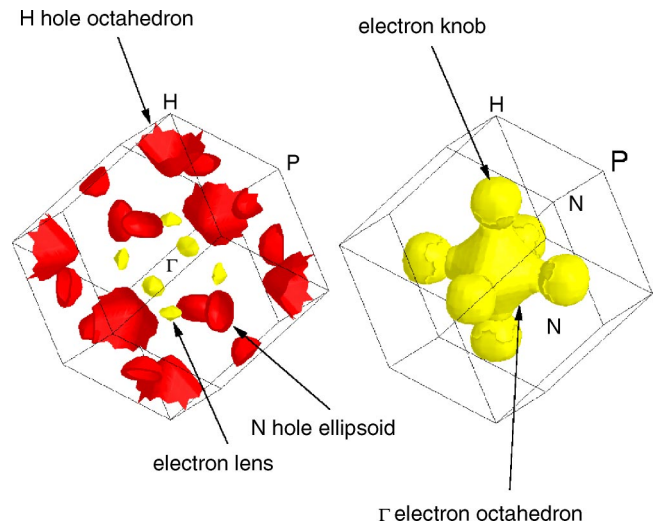


FIG. 1. (Color online) The calculated FS of pure Cr, showing (left) the hole sheet (dark) and the small electron lenses along Γ - H (light), and (right) the electron “jack” (octahedron with knobs).

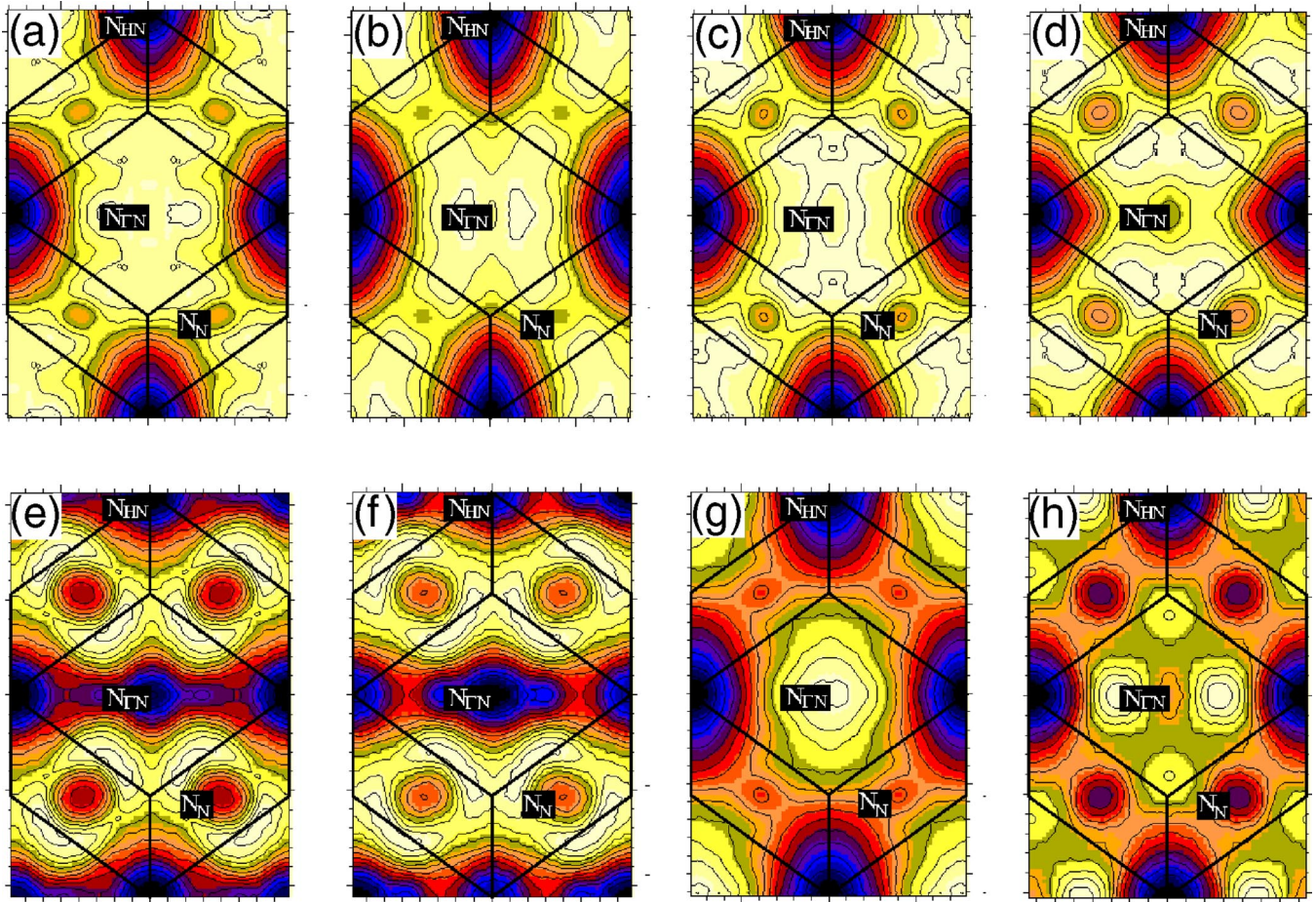


FIG. 2. (Color online) Evolution of the FS projected along [110] from LCW-folded BZ occupancies for (a) Cr, (b) $\text{Cr}_{0.95}\text{V}_{0.05}$, (c) $\text{Cr}_{0.85}\text{V}_{0.15}$, (d) $\text{Cr}_{0.7}\text{V}_{0.3}$, (e) $\text{Cr}_{0.25}\text{V}_{0.75}$, (f) V, (g) $\text{Cr}_{0.85}\text{Mo}_{0.15}$, and (h) Mo. The occupancies are represented on a grayscale intensity plot, where the lighter shades correspond to higher occupancy. The labels refer to the symmetry points which along the [110] direction are projected onto each other. The N -hole ellipsoids can be identified as areas of low occupancy (dark shades), where along the [110] direction the N point is projected onto itself (N - N).

+ \mathbf{G}), where an electron band crosses the Fermi level E_F . Tomographic methods can be used to reconstruct the full 3D momentum density from a series of measured 2D projections.¹⁸ When the FS is of paramount interest, the Lock-Crisp-West procedure¹⁹ (“LCW-folding”) is often followed. Here the various FS discontinuities are superimposed by folding $\rho(\mathbf{p})$ (or its measured projections) back into the first Brillouin zone (BZ). The result is a new \mathbf{k} -space density, which aside from a modulating factor (usually a weak function of \mathbf{k}) is simply the electron occupation density (or its projection along the spectrometer axis). The FS topology can then be extracted by using a “zero-contour” edge-detection method based on maximum-entropy deconvolution, and described fully in Refs. 20 and 21. This well-established technique has recently been used by some of the present authors to determine the FS topology and identify nesting features in a wide range of systems.^{21–23} The virtue of the 2D-ACAR technique in such studies is that it reveals *directly* the shape of the FS.

To assist in our analysis, momentum densities were calculated using the linearized muffin-tin orbital (LMTO) method within the atomic sphere approximation, including

combined-correction terms.^{24,25} In addition, self-consistent Korringa-Kohn-Rostoker calculations of the alloy electronic structures were made within the coherent potential approximation (KKR-CPA).²⁶

The results presented here comprise three complementary sets of analyses. First, the [110] 2D-ACAR projections for a wide range of compositions of $\text{Cr}_{1-x}\text{V}_x$ and $\text{Cr}_{1-x}\text{Mo}_x$ alloys were measured and the obtained LCW-folded distributions are shown in Fig. 2. This demonstrates the evolution of the various FS features, especially the N -hole ellipsoids (since N projects onto N along the [110] direction and thus this feature is unobscured), which can be seen to evolve in both shape and size when Cr is alloyed with V and Mo. Also, as predicted by the KKR-CPA calculations,¹⁶ they remain a well-defined feature in spite of the substitutional disorder.

Investigating the evolution of the size of the N -hole ellipsoids in projection (Fig. 2) provides us with a trend in shape and size across the different concentrations, but it is not sufficient for determining the actual size of this FS feature, since only an average caliper (averaged over the ellipsoid) can be extracted. For an investigation of the FS dimensions it is therefore necessary to tomographically reconstruct the full

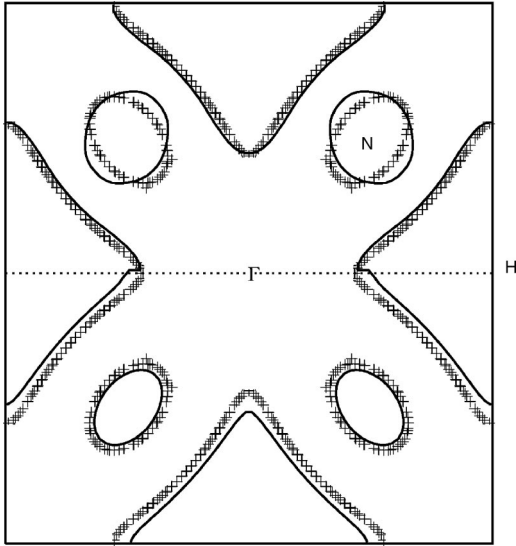


FIG. 3. The holelike FS (octahedra at H and pockets at N) of $\text{Cr}_{0.7}\text{V}_{0.3}$ in the (100) plane. The solid lines represent the FS obtained using the zero-contour method on the reconstructed experimental data (top half of figure) and from the fit to the anisotropy of the LMTO electron-positron momentum density (bottom half of figure). The crosses are the KKR-CPA calculation for this composition, and the size of each cross indicates the amount by which the FS is smeared out in \mathbf{k} space due to the substitutional disorder (Ref. 35).

3D momentum densities and LCW-folded occupancies in the first BZ. In our second analysis we carried out such a full reconstruction from a series of projections (5–6) for three particular compositions, viz., pure Cr, $\text{Cr}_{0.7}\text{V}_{0.3}$, and $\text{Cr}_{0.85}\text{Mo}_{0.15}$.²⁷ The FS was then extracted and is shown for $\text{Cr}_{0.7}\text{V}_{0.3}$ in the top half of Fig. 3, along with our KKR-CPA calculation. The agreement of this contour with the shape of the KKR-CPA H -hole octahedron is excellent. The implication is that the topology of the octahedron is well described by the LDA calculations, an important result given the recent interest in $\text{Cr}_{1-x}\text{V}_x$ as a nested system close to a quantum critical point.²⁸ However, there is an important disagreement in the shape of the ellipsoids which, in the reconstructed density, appear much more spherical than the calculation predicts, a result supported by previous Compton scattering measurements.²⁹

It has previously been suggested that a rigid-band model can be meaningfully applied to the electronic structure of $\text{Cr}_{1-x}\text{V}_x$ alloys.¹⁴ With this assertion in mind, in our final analysis procedure, FS topologies were directly obtained from the measurements of Cr, $\text{Cr}_{0.7}\text{V}_{0.3}$, and V by applying a fitting procedure of the calculated electron-positron momentum density to the data. In this procedure the three partially occupied electron bands from the LMTO calculation are allowed to be populated up to a different Fermi energy, and for each shift of E_F the corresponding electron-positron momentum density is determined. Since the FS information is contained in the anisotropic part of $\rho(\mathbf{p})$, the so-called radial anisotropy $R(p_x, p_y)$ is constructed by subtracting from the data [a 2D projection of $\rho(\mathbf{p})$, $N(p_x, p_y)$] its radial average, i.e.,

$$R(p_x, p_y) = N(p_x, p_y) - \overline{N(p_x, p_y)} \Big|_{p=\text{const}}. \quad (1)$$

This quantity is very sensitive to the position of the Fermi level within each band (and through these to the FS topology) and thus by simultaneously fitting the radial anisotropies of the calculated spectra to those of all the measured projections for a particular composition, a set of rigid-band shifts was obtained, which corresponded to the best agreement between the calculated and measured FS topologies. The details of the procedure can be found in Ref. 30. As a check, the occupied fractions of the BZ for the shifted bands were correct to better than 0.02 electrons. Moreover, in V, the resultant Fermi level shifts significantly improved the agreement of the ellipsoid areas with de Haas–van Alphen (dHvA) experiments,³¹ with the original LMTO calculation overestimating them by more than 10%, and our fit underestimating by just over 1%. The extremal FS vectors originating from the fit could be directly extracted from the shifted band structure. The fitted FS of $\text{Cr}_{0.7}\text{V}_{0.3}$ is shown in the bottom half of Fig. 3. The shape of the H -hole octahedron is almost identical to that predicted by the KKR-CPA (and the zero contour from the reconstruction in the top half of Fig. 3). Although the N -hole ellipsoid strongly resembles the KKR-CPA prediction (indicating how rigid-band-like the electronic structure is), there is of course disagreement with the zero contour from the reconstruction, since the rigid-band mechanism only allows for the shape of the ellipsoids to change in a restricted manner. It is particularly interesting that as a result of this rigid-band fitting procedure the “lens” (the small electron pocket inside the knob of the electron jack along Γ - H) was detected. This is the first time, to our knowledge, that this FS sheet has been seen in a positron annihilation experiment. The fit results show that the lens is still present at a V concentration of 30%, whereas calculations suggest it should have disappeared.¹⁴ The size of the lens had earlier made it a popular source of the 18 Å period in multilayers with Cr.^{8,10,32} However, as calculations predicted that it disappears at V concentrations of around 15% (Ref. 14) its popularity waned in favor of the N -hole pockets. Even though the current results show that it is robust (as far as 30% V), it certainly does not get any larger which would be necessary to explain the decrease in period. Moreover, the other factors counting against it (i.e., the low joint density of states for the lens and its pure d character^{12–14}) still apply. The positron experiment is not able to resolve the character of the states on the FS, but our calculations are in agreement with other studies (e.g. Ref. 14) in indicating the pure d character of the lens and the p - d character ($\approx 10\%$ s , 70% p , and 20% d , and rather insensitive to the alloy concentration) of the N -hole ellipsoids.

A summary of the oscillation periods corresponding to the various calipers obtained from the reconstructions and rigid-band fitting procedures, together with the multilayer periods for alloys with V and Mo (taken from Lathiotakis *et al.*^{16,33}), are plotted in Figs. 4 and 5. The KKR-CPA calculations of Lathiotakis *et al.*¹⁶ have indicated that extremal vectors along N - H and N - Γ both evolve in a manner which is qualitatively in agreement with the observed [110] oscillation periods,⁹ with the N - H caliper also agreeing quantitatively.

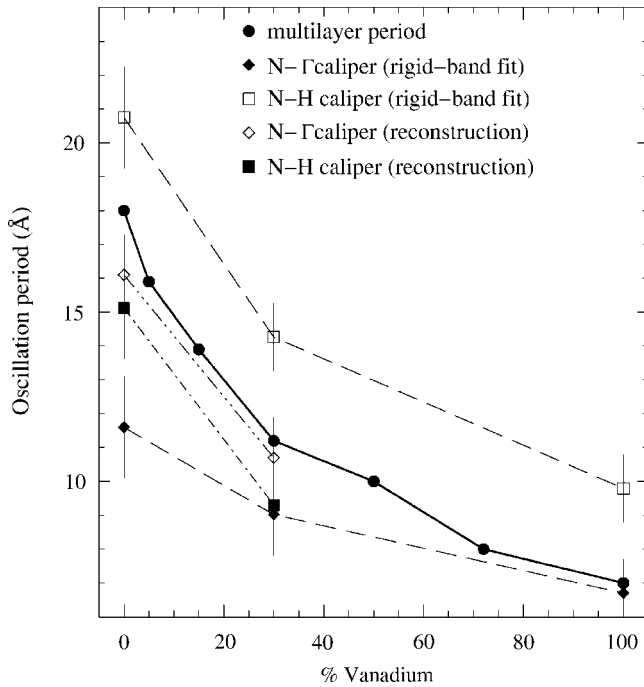


FIG. 4. Evolution of the oscillation period in the $\text{Fe}/\text{Cr}_{1-x}\text{V}_x/\text{Fe}$ multilayer system (data are taken from Ref. 16), and from the calipers of the N -hole ellipsoids along different directions.

Contrary to these calculations, our data show that the ellipsoid axis N - H is larger than N - Γ , and under alloying N - H eventually becomes smaller than N - Γ . It is worth noting that for geometric reasons the dHvA experiments^{31,34} are unable to determine which is the larger axis. This evolution strongly suggests that the N - Γ caliper could be associated with the oscillation period. Since the calculated band structure at high Cr concentrations predicts a different shape for the N -hole ellipsoids from the experiment (Fig. 3), and given the dominant influence of the hole octahedron and electron jack in determining the anisotropy, the rigid-band analysis can only indicate the trend. However, in V where the experimental ellipsoid orientation is in accord with calculation and its area in excellent agreement with dHvA experiment,³¹ the Γ - N caliper closely matches the multilayer period (Fig. 4).

The shortening of the observed oscillation period in the $\text{Cr}_{1-x}\text{Mo}_x$ alloy series has previously been something of an enigma. Lathiotakis *et al.*³³ have suggested that owing to the large lattice constant mismatch between Fe (2.867 Å) and

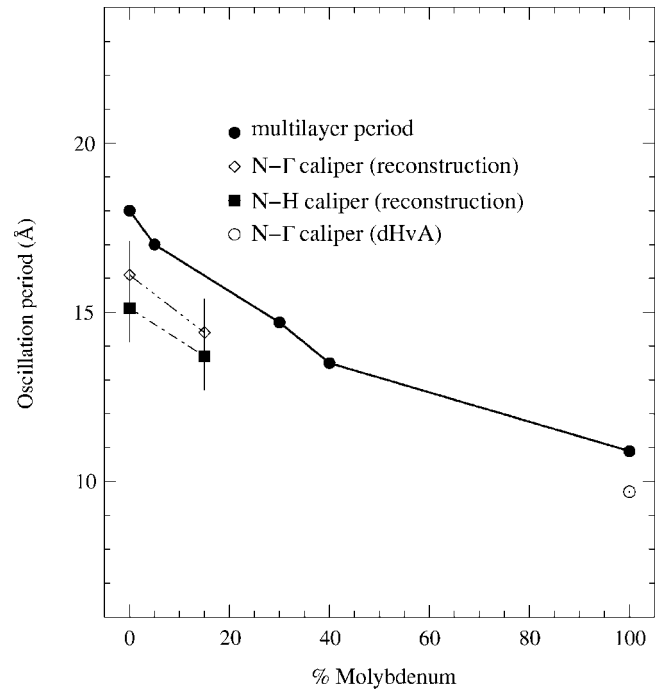


FIG. 5. Evolution of the oscillation period in the $\text{Fe}/\text{Cr}_{1-x}\text{Mo}_x/\text{Fe}$ multilayer system (data are taken from Ref. 33), and from the calipers of the N -hole ellipsoids along different directions from 2D-ACAR measurements and dHvA experiments (data from Ref. 36).

Mo (3.148 Å), the structure of the alloy is likely to be distorted. They showed that agreement between the oscillation periods and the N -hole ellipsoid evolution could be achieved if they performed all their KKR-CPA calculations at the Fe lattice constant. However, our results suggest that the evolution of the experimentally measured FS with increasing Mo concentration is sufficient to explain the trend.

In conclusion, the FS topologies of a series of Cr-V and Cr-Mo alloys have been investigated in order to detect the particular piece thought, through its nesting, to be responsible for the oscillatory exchange coupling in $\text{Fe}/\text{Cr}_{1-x}\text{V}_x/\text{Fe}$ and $\text{Fe}/\text{Cr}_{1-x}\text{Mo}_x/\text{Fe}$ multilayers. The evolution of the N - Γ caliper of the N -hole ellipsoids is shown to correlate closely with the experimentally observed periods.

We wish to thank A.A. Manuel for making his data ($\text{Cr}_{0.25}\text{V}_{0.75}$) available. We acknowledge the financial support of the UK EPSRC and the Royal Society (S.B.D.).

¹P. Grünberg, R. Schreiber, Y. Pang, M.B. Brodsky, and H. Sowers, Phys. Rev. Lett. **57**, 2442 (1986).

²M.N. Baibich, J.M. Broto, A. Fert, F. Nguyen Van Dau, F. Petroff, P. Etienne, G. Creuzet, A. Friederich, and J. Chazelas, Phys. Rev. Lett. **61**, 2472 (1988); G. Binasch, P. Grünberg, F. Saurenbach, and W. Zinn, Phys. Rev. B **39**, 4828 (1989).

³S.S.P. Parkin, N. More, and K.P. Roche, Phys. Rev. Lett. **64**, 2304 (1990); S.S.P. Parkin, R. Bhadra, and K.P. Roche, *ibid.* **66**, 2152 (1991); S.S.P. Parkin, *ibid.* **67**, 3598 (1991).

⁴P. Bruno and C. Chappert, Phys. Rev. Lett. **67**, 1602 (1991); P. Bruno and C. Chappert, Phys. Rev. B **46**, 261 (1992).

⁵D.M. Edwards, J. Mathon, R.B. Muniz, and M.S. Phan, Phys. Rev. Lett. **67**, 493 (1991); M.D. Stiles, Phys. Rev. B **48**, 7238 (1993); P. Bruno, J. Phys.: Condens. Matter **11**, 9403 (1999).

⁶N.N. Lathiotakis, B.L. Györfy, and B. Újfalussy, Phys. Rev. B **61**, 6854 (2000); N.N. Lathiotakis, B.L. Györfy, E. Bruno, and B. Ginatempo, *ibid.* **62**, 9005 (2000).

⁷E. Fawcett, Rev. Mod. Phys. **60**, 209 (1988).

- ⁸D. Li, J. Pearson, S.D. Bader, E. Vescovo, D.-J. Huang, P.D. Johnson, and B. Heinrich, *Phys. Rev. Lett.* **78**, 1154 (1997).
- ⁹M. van Schilfhaarde, F. Herman, S.S.P. Parkin, and J. Kudrnovsky, *Phys. Rev. Lett.* **74**, 4063 (1995).
- ¹⁰D.D. Koelling, *Phys. Rev. B* **50**, 273 (1994).
- ¹¹S. Mirbt, A.M.N. Niklasson, B. Johansson, and H.L. Skriver, *Phys. Rev. B* **54**, 6382 (1996).
- ¹²M.D. Stiles, *Phys. Rev. B* **54**, 14 679 (1996).
- ¹³L. Tsetseris, B. Lee, and Y.-C. Chang, *Phys. Rev. B* **55**, 11 586 (1997); **56**, 11 392 (1997).
- ¹⁴D.D. Koelling, *Phys. Rev. B* **59**, 6351 (1999).
- ¹⁵C.-Y. You, C.H. Sowers, A. Inomata, J.S. Jiang, S.D. Bader, and D.D. Koelling, *J. Appl. Phys.* **85**, 5889 (1999).
- ¹⁶N.N. Lathiotakis, B.L. Györfy, E. Bruno, B. Ginatempo, and S.S.P. Parkin, *Phys. Rev. Lett.* **83**, 215 (1999).
- ¹⁷R.N. West, in *Positron Spectroscopy of Solids*, Proceedings of the International School of Physics "Enrico Fermi," Course CXXV, Varenna, 1993, edited by A. Dupasquier and A.P. Mills, Jr. (IOS Press, Amsterdam, 1995), p 75.
- ¹⁸A.M. Cormack, *J. Appl. Phys.* **34**, 2722 (1963); **35**, 2908 (1964); G. Kontrym-Sznajd, *Phys. Status Solidi A* **117**, 227 (1990).
- ¹⁹D.G. Lock, V.H.C. Crisp, and R.N. West, *J. Phys. F: Met. Phys.* **3**, 561 (1973).
- ²⁰S.B. Dugdale, M.A. Alam, H.M. Fretwell, M. Biasini, and D. Wilson, *J. Phys.: Condens. Matter* **6**, L435 (1994).
- ²¹S.B. Dugdale, H.M. Fretwell, M.A. Alam, G. Kontrym-Sznajd, R.N. West, and S. Badrzadeh, *Phys. Rev. Lett.* **79**, 941 (1997); H.M. Fretwell, S.B. Dugdale, M.A. Alam, D.C.R. Hedley, A. Rodriguez-Gonzalez, and S.B. Palmer, *ibid.* **82**, 3867 (1999).
- ²²S.B. Dugdale, M.A. Alam, I. Wilkinson, R.J. Hughes, I.R. Fisher, P.C. Canfield, T. Jarlborg, and G. Santi, *Phys. Rev. Lett.* **83**, 4824 (1999).
- ²³I. Wilkinson, R.J. Hughes, Zs. Major, S.B. Dugdale, M.A. Alam, E. Bruno, B. Ginatempo, and E.S. Giuliano, *Phys. Rev. Lett.* **87**, 216401 (2001).
- ²⁴O.K. Andersen, *Phys. Rev. B* **12**, 3060 (1975); T. Jarlborg and G. Arbman, *J. Phys. F: Met. Phys.* **7**, 1635 (1977).
- ²⁵A.K. Singh and T. Jarlborg, *J. Phys. F: Met. Phys.* **15**, 727 (1985).
- ²⁶E. Bruno and B. Ginatempo, *Phys. Rev. B* **55**, 12 946 (1997).
- ²⁷It was not possible to carry out a full 3D reconstruction for all different compositions mentioned in this paper owing to time constraints of the experiment ($\approx 4-6$ months per sample).
- ²⁸A. Yeh, Y.-H. Soh, J. Brooke, G. Aeppli, T.F. Rosenbaum, and S.M. Hayden, *Nature (London)* **419**, 459 (2002); M.R. Norman, Q. Si, Ya.B. Bazaliy, and R. Ramazashvili, *Phys. Rev. Lett.* **90**, 116601 (2003); C. Pépin and M.R. Norman, *Phys. Rev. B* **69**, 060402 (2004).
- ²⁹Y. Tanaka, K.J. Chen, C. Bellin, G. Louprias, H.M. Fretwell, A. Rodrigues-Gonzalez, M.A. Alam, S.B. Dugdale, A.A. Manuel, A. Shukla, T. Buslaps, P. Suortti, and N. Shiotani, *J. Phys. Chem. Solids* **61**, 365 (2000).
- ³⁰Zs. Major, S.B. Dugdale, R.J. Watts, J. Laverock, J.J. Kelly, D.C.R. Hedley, and M.A. Alam, *J. Phys. Chem. Solids* (to be published).
- ³¹R. Parker and M. Halloran, *Phys. Rev. B* **9**, 4130 (1974).
- ³²E.E. Fullerton, J.E. Mattson, C.H. Sowers, and S.D. Bader, *Scr. Metall. Mater.* **33**, 1637 (1995).
- ³³N.N. Lathiotakis, B.L. Györfy, B. Ginatempo, and E. Bruno, *J. Magn. Magn. Mater.* **198-199**, 447 (1999).
- ³⁴J.E. Graebner and J.A. Marcus, *Phys. Rev.* **175**, 659 (1968).
- ³⁵E. Bruno, B. Ginatempo, E.S. Giuliano, A.V. Ruban, and Yu.Kh. Vekilov, *Phys. Rep.* **249**, 353 (1994).
- ³⁶J.B. Ketterson, D.D. Koelling, J.C. Shaw, and L.R. Windmiller, *Phys. Rev. B* **11**, 1447 (1975).